

# New Chromium Complexes for Ethylene Oligomerization: Extended Use of Tridentate Ligands in Metal-Catalyzed Olefin Polymerization

Brooke L. Small,<sup>\*,†</sup> Michael J. Carney,<sup>‡</sup> Danah M. Holman,<sup>‡</sup> Colleen E. O'Rourke,<sup>‡</sup> and Jason A. Halfen<sup>‡</sup>

Chevron Phillips Chemical Company, LP, 1862 Kingwood Drive, Kingwood, Texas 77339, and Department of Chemistry, University of Wisconsin–Eau Claire, 105 Garfield Avenue, Eau Claire, Wisconsin 54702

Received October 15, 2003; Revised Manuscript Received April 6, 2004

**ABSTRACT:** A family of chromium complexes bearing tridentate pyridine-based ligands are disclosed as highly active precatalysts for the oligomerization of ethylene. The ligands are comprised of two distinct types: Type 1, in which both ketone groups of 2,6-diacetylpyridine are converted to imines to produce pyridine bisimine NNN ligands; and Type 2, in which only one ketone group of 2,6-diacetylpyridine is condensed with an aniline derivative to give monoimine NNO coordination sets. Ligands of either type are coordinated to chromium(II) or chromium(III) chlorides, and activation of the resultant complexes with methylaluminoxane (MAO) produces highly active ethylene oligomerization and polymerization catalysts. Catalysts of Type 1 (NNN set) generally produce 1-butene when only two *ortho* alkyl substituents are present but switch to making waxes or polyethylene when the size and/or number of *ortho* substituents are increased. Catalysts of Type 2 (NNO set) produce waxes and polyethylene under all of the substitution patterns studied. The butene-producing catalysts can make 1-butene with 99.5+% purity, and the wax-producing catalysts make highly linear to moderately branched waxes, depending on the presence of an  $\alpha$ -olefin comonomer.

## Introduction

The development of homogeneous chromium-based catalysts for olefin polymerization has received considerable attention,<sup>1</sup> spurred by the extensive use of chromium catalysts in commercial ethylene polymerization.<sup>2</sup> Seemingly at the interface of late-transition-metal and early-metal metallocene catalysts, chromium has been used in a number of different polymerization studies, employing cyclopentadienyl-type ligands, non-Cp ligands possessing heteroatom donor sets and various mixed systems. Figure 1 provides an overview of some recently reported homogeneous chromium catalysts.

As can be seen from Figure 1, the complexes vary not only in their structures, but also in oxidation state (+2 vs +3), formal electron count, and overall charge (neutral vs cationic).<sup>3</sup> Furthermore, although it is reasonable that more electrophilic cationic systems should exhibit higher activities than neutral ones, correlations between chromium oxidation state (or formal electron count) and catalyst productivity are vague at best. For example, neutral catalysts **A** and **B**, reported by Theopold,<sup>4</sup> and **C**, reported by Carney,<sup>5</sup> have relatively low activities, but potentially cationic (after MAO activation) complexes **D**, **E**, and **F** are only marginally more active.<sup>1,6</sup> Since **D** only has only two nitrogen donors, the catalyst might be too electron deficient. Using this line of reasoning, one might expect that tridentate monoanionic ligands would yield more active catalysts. However, complex **G**, containing a tridentate monoanionic ligand, only exhibits moderate polymerization activity.<sup>7</sup> One of the more promising

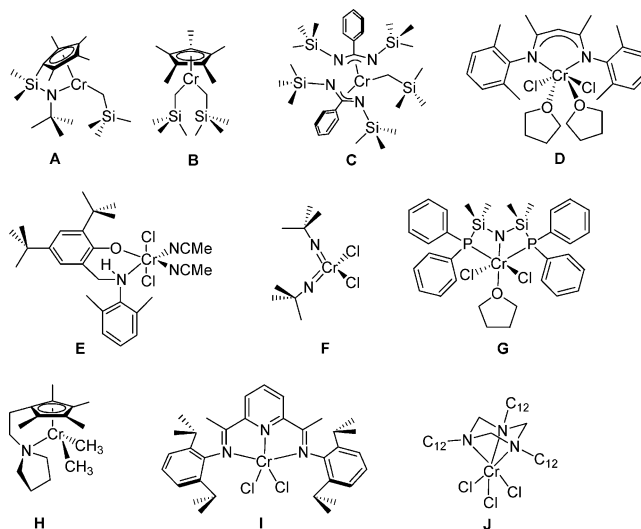


**Figure 1.** Selected examples of homogeneous chromium-based polymerization catalysts. In each example the reported precatalyst structure is shown. Many of these complexes require an alkylating cocatalyst in order to achieve activation. Speculation on the nature of the active species for each system is well beyond the intent of this work.

results in homogeneous chromium catalysts, complex **H**, was recently reported by Jolly,<sup>8</sup> who disclosed that by changing the well-known 'constrained geometry' ligand's anionic amido ligand to a neutral amine, highly active cationic chromium(III) catalysts could be produced upon activation with MAO.

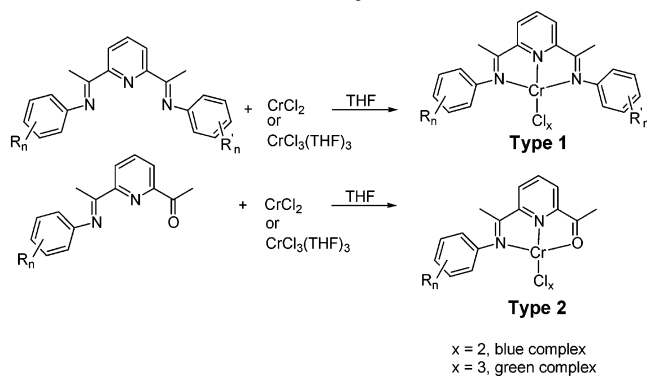
The performance of type **H** catalysts seems to indicate that cationic chromium(III) complexes with carefully chosen monoanionic ligands might be the best alternative for homogeneous chromium systems. Complex **I**, though recently reported to polymerize propylene with modest rates,<sup>9</sup> caused us to further consider this issue of catalyst design. Ethylene polymerization data for **I**

\* To whom correspondence should be addressed. E-mail: small-bl@cpchem.com.

<sup>†</sup> Chevron Phillips Chemical Co.

<sup>‡</sup> University of Wisconsin–Eau Claire.

### Scheme 1. Preparation of Chromium-Based Precatalysts



Complex	R <sub>n</sub>	R' <sub>n</sub>
1	Unsubst.	Unsubst.
2	2-Me	2-Me
3	2-Et	2-Et
4	2- <i>i</i> Pr	2- <i>i</i> Pr
5	2- <i>t</i> Bu	2- <i>t</i> Bu
6	2,6-Me <sub>2</sub>	2,6-Me <sub>2</sub>
7	2,5- <i>t</i> Bu <sub>2</sub>	2,5- <i>t</i> Bu <sub>2</sub>
8	2,6-Me <sub>2</sub>	N.A.
9	2,6- <i>i</i> Pr <sub>2</sub>	N.A.
10	2- <i>t</i> Bu	N.A.
11	2,4,6-Me <sub>3</sub>	4- <i>t</i> Bu
12	2,4,6-Me <sub>3</sub>	2-Me
13	2,4,6-Me <sub>3</sub>	2-Et
14	2,6- <i>i</i> Pr <sub>2</sub>	2,6- <i>i</i> Pr <sub>2</sub>

were not reported in ref 9, but since even chromium(II) chloride, when activated with MAO, shows some intrinsic ability to polymerize ethylene, we expected that complexes of type **1** would display some activity for ethylene polymerization. Additionally, complexes such as **J**, which like **I** also bear tridentate neutral ligands, yield relatively high activity polymerization catalysts.<sup>10</sup> During the preparation of our manuscript, Esteruelas et al. reported the synthesis of pyridine bisimine chromium(III) complexes for the polymerization of ethylene.<sup>11a</sup> Our studies augment this recent publication by focusing on previously unreported chromium complexes supported by substituted and asymmetric tridentate pyridine bisimine and monoimine ligands. The products made by these chromium complexes vary dramatically from those reported by Esteruelas, ranging from 1-butene to heavy waxes and polyethylene. Moreover, our results conclusively demonstrate that both chromium(II) and chromium(III) complexes produce highly active catalysts for the oligomerization and polymerization of ethylene.<sup>11b</sup>

### Results and Discussion

Tridentate pyridine bisimine ligands, which were first reported many years ago in the chemical literature,<sup>12</sup> have been much more recently documented as key components in the preparation of highly active iron- and cobalt-based catalysts for olefin polymerization.<sup>13</sup> The iron and cobalt precatalysts are easily prepared in high yields by stirring a suspension of the ligand and the appropriate metal salt in either hot *n*-butanol or THF. Similarly, the analogous chromium precatalysts may be prepared by simply stirring a suspension of CrCl<sub>2</sub> or CrCl<sub>3</sub>(THF)<sub>3</sub> with the tridentate ligand in hot THF (Scheme 1). In addition to the bisimine complexes (Type 1) of Scheme 1, tridentate complexes of Type 2, in which one of the ketone groups is not converted to an imine, can also be prepared.<sup>14</sup>

The chromium(II) complexes are blue or violet in color, whereas the chromium(III) complexes are green.

The majority of the polymerizations in this report were carried out using the chromium(II) analogues of both Type 1 and Type 2. The chromium(II) derivatives are air-sensitive, making them difficult to isolate in analytically pure form. Indeed, on occasion we have noted that small amounts of oxygen contamination during isolation of the chromium(II) species results in green products, presumably due to oxidation to chromium(III). We have, however, obtained satisfactory elemental analyses for the chromium(III) complexes, and these results are shown in Table 6. In any event, the data and discussion to follow will show that the chromium(II) and chromium(III) complexes possess nearly identical activities, as well as likely identical active site structures. The chromium(II) complexes in this report are numbered sequentially, and the chromium(III) analogues are identified by the same numbers followed by the "prime" superscript, e.g., **2'**.

**Discussion of Polymerization Data.** When complexes of either Type 1 or Type 2 (Scheme 1) are activated with modified methylalumoxane (MMAO),<sup>15</sup> remarkably active catalysts—from both the chromium(II) and chromium(III) precursors—are generated for the oligomerization and polymerization of ethylene. Table 1, which includes representative data, illuminates several interesting features of these new systems. Analysis of the data for catalysts of Type 1, shown in entries 1–9, indicates a sizable effect on catalyst activity with increasing ligand steric bulk. However, the effect is far from regular. In fact, it should be noted that the widely differing activities exhibited by catalysts **1**–**13** made it difficult to run all of the reactions under identical conditions (catalyst amount, pressure, temperature, Al:Cr ratio). In the paragraphs that follow, we have been careful to only discuss and directly compare catalysts run under comparable reaction conditions. For example, experiments 1–4 all exhibited rapid exotherms from room temperature to 35 °C (indicating high catalyst activity) upon catalyst activation under 1.0 bar of ethylene, but the reaction involving the 2-*tert*-butyl-substituted complex **5** (entry 5) did not exceed room temperature during the course of the reaction. In entry 6, complex **6**, bearing four *ortho* methyl substituents, caused a large exotherm and polymerized ethylene with approximately five times higher productivity than **5**, as evidenced by the respective product yields.

This observation indicates that large *tert*-butyl groups in two *ortho* positions (the 2-position of each aryl ring) have a more detrimental effect on activity (presumably steric in origin) than methyl groups in all four *ortho* positions. However, entries 7 and 8, in which the 2-*tert*-butyl and 2,5-di-*tert*-butyl complexes **5** and **7** are compared under identical reaction pressure and Al:Cr ratio, clearly show that steric arguments alone cannot rationalize Type 1 catalyst activity.<sup>16</sup> Comparing entries 7 and 8, complex **7** with 2,5-di-*tert*-butyl substituents shows a high activity relative to complex **5** (the higher reaction temperature of 100 °C in experiment 8 is due to the catalyst exotherm). The relationship between the increased activity and the presence of an additional *tert*-butyl group in the 5-position of the aryl rings is not yet understood. Increasing ethylene pressure also dramatically increases catalyst activity, as shown by comparing entries 2 and 9 (catalyst **2**). At 27 bar of ethylene, catalyst activation at room temperature results in a very rapid exotherm to 80 °C. The temperature was maintained in this reaction by internal cooling, and even

Table 1. Selected Data for the Polymerization of Ethylene and  $\alpha$ -Olefins Using Chromium(II) Complexes

entry	complex	cat. amt. (mg)	Al:Cr <sup>a</sup>	P <sub>C2</sub> (bar), com.(amt.) <sup>b</sup>	rxn length (min)	T (°C) <sup>c</sup>	Yield (g)	Prod. <sup>d</sup> (g/g Cr complex)	major products/notes <sup>e</sup>	GPC data (MW <sub>peak</sub> × 10 <sup>3</sup> ) <sup>f</sup>
1	<b>1</b>	5.7	500	1.0	30	35	n.d.	n.d.	2-butene	n.d.
2	<b>2</b>	6.1	500	1.0	60	35	n.d.	n.d.	1-butene	n.d.
3	<b>3</b>	5.4	500	1.0	80	35	n.d.	n.d.	1-butene	n.d.
4	<b>4</b>	4.6	500	1.0	30	35	n.d.	n.d.	1-butene	n.d.
5	<b>5</b>	5.2	500	1.0	180	25	1.9	370	wax/PE	0.72
6	<b>6</b>	6.7	500	1.0	120	35	10.4	1550	wax/PE	0.83
7	<b>5</b>	5.0	500	27	30	60	19.9	4000	wax/PE	0.17
8	<b>7</b>	5.0	500	27	30	100	57.3	11 500	PE	11.0
9	<b>2</b>	5.0	500	27	30	80	n.d.	n.d.	1-butene	40.0
10	<b>8</b>	18.0	160	1.0	180	25	6.0	330	PE (Figure 6b)	34.0
11	<b>9</b>	21.0	160	1.0	180	25	1.2	60	PE	68.2
12	<b>10</b>	6.3	500	1.0	60	25	1.1	180	PE	103
13	<b>8</b>	5.0	1150	27	60	80	101	20 200	wax/PE (Figure 6a)	1.54
14	<b>8</b>	4.0	1150	27	60	100	95.0	23 800	wax/PE	1.20
15	<b>9</b>	10.0	1150	27	60	45	4.9	1490	wax/PE	0.98
16	<b>8</b>	13.6	260	1.0, 1-hexene	180	25	22.2	1520	wax/PE (Figure 6c)	0.85
17	<b>11</b>	3.0	500	1.0	30	40	n.d.	n.d.	1-butene	0.35
18	<b>12</b>	4.0	1000	27	30	60	70.0	17 500	linear $\alpha$ -olefins, K = 0.60	0.15
19	<b>13</b>	4.0	1000	27	30	60	45.0	11 300	linear $\alpha$ -olefins, K = 0.65	0.16

<sup>a</sup> Molar ratio of Al to Cr in the reaction. <sup>b</sup> Ethylene pressure and amount of comonomer present (entry 16). For entry 16, the 1-hexene was introduced as a 1:5 v:v mixture in *n*-heptane. <sup>c</sup> Temperatures shown are the maximum values reached due to the heat generated by the reaction. <sup>d</sup> Prod. = productivity, which was not determined for reactions in which the major product was butene. <sup>e</sup> All of the reactions produced small to moderate amounts of polyethylene byproducts. The reactions were run in *n*-heptane or cyclohexane. <sup>f</sup> GPC data are for the isolated solid fraction of the product. Bimodal behavior, whether solely due to chain transfer to aluminum or the presence of multiple catalyst active sites, makes the values for  $M_w/M_n$  less useful than the more straightforward peak molecular weights of the key GPC signals. GPC traces can be found in the Supporting Information. Table 2 and Figure 3 illustrate the effect of changing activator concentration.

though the amount of product was not accurately quantified due to its volatility (butene), the degree of the exotherm indicated that the turn-over frequency (TOF) was likely approaching 10<sup>6</sup> mol ethylene/mol cat·h (productivity > 50 000 g of product/g of Cr complex). Gas chromatography showed this butene to be very high purity 1-butene, at least 99% within the C<sub>4</sub> fraction, with traces of hexene and octene present. In addition to these olefins, a significant amount of polyethylene was also produced. Due to the butene volatility, it was not possible to determine the exact amounts of each product. However, the polyethylene coproduct was analyzed by gel-permeation chromatography (see Table 1), and the molecular weight data are discussed in the following section.

The catalysts in entries 1–8, in addition to possessing widely varying activities, also produce a highly divergent product slate. Methyl-, ethyl-, and isopropyl-substituted catalysts (entries 2–4) make predominantly high-purity 1-butene (>99%, with polyethylene coproduct), but entry 1, using the unsubstituted complex **1**, produces mainly 2-butene, via isomerization of 1-butene.<sup>17</sup> The product composition becomes even more curious upon comparing entries 1–4 to entry 5. While entries 1–4 all result in butene production, the 2-*tert*-butyl catalyst **5** makes only waxes and polyethylene. Furthermore, catalyst **6** (entry 6), bearing four *ortho* methyl groups, makes waxes and polyethylene as the major products. The effects of minor substituent changes on product molecular weight have been well-documented in tridentate pyridine bisimine iron and cobalt catalysts as have the substituent effects for  $\alpha$ -diimine-based nickel and palladium systems.<sup>13,18</sup> In general, increasing the steric bulk at the 2- and 6-positions of the imino-aryl rings results in higher molecular weight, but the drastic effect on product molecular weight by slight ligand modifications in these chromium catalysts is unusual.

As with Type 1 complexes, catalyst activity for the Type 2 systems is largely dependent on the size of the

*ortho* substituents of the imino-aryl ring (Note: for Type 2 complexes, there is only one ring to consider). Entry 10, employing complex **8** with two methyl groups, shows a much higher activity than either catalyst **9** with two isopropyl groups (entry 11) or catalyst **10** with a single *tert*-butyl group (entry 12). This trend is also seen at higher pressures (entries 13 and 14 vs 15) as **8** remains much more active than **9**.

In addition to their ability to rapidly oligomerize ethylene, these new chromium catalysts are capable of incorporating comonomers. Entry 16, in which dimethyl-substituted **8** was used, demonstrates the ability of these systems to form ethylene/ $\alpha$ -olefin copolymers. The branched wax produced in entry 16, run in a 1:5 1-hexene:heptane v:v ratio, indicates substantial comonomer incorporation, as demonstrated by examining the copolymers via gas chromatography. Figure 2 shows a comparison of the waxes made by catalyst system **8** in entries 10, 13, and 16. Entry 13, in which elevated ethylene pressure was used and no comonomer was employed, shows only very low levels of branching. The wax from experiment 10 is again mostly linear, with the slightly increased level of branching due to the use of lower ethylene pressure (product reincorporation likely becomes more competitive with ethylene insertion). Entry 16, in which 1-hexene comonomer was added, shows high levels of branching, thus conclusively demonstrating the ability to incorporate comonomer. Worth noting, these GC traces only show the low-molecular-weight (<1000) portions of the polymer samples. For entries 10, 13, and 16, the GC traces represent about 15%, 40%, and 50%, respectively, of the total polymer formed. GPC data are discussed in the following section.

Further comparisons between Type 1 and Type 2 catalysts highlight other differences between these chromium systems. For example, upon comparing entry 2 (Type 1) to entry 10 (Type 2), the primary product changes from 1-butene to linear wax as illustrated in Scheme 2. The observation that the Type 2 ketone-

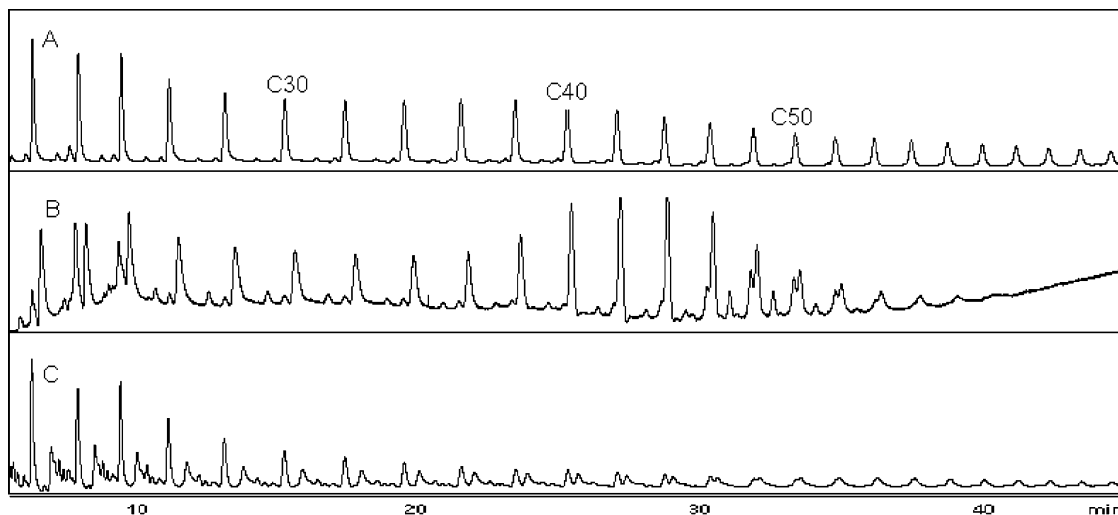
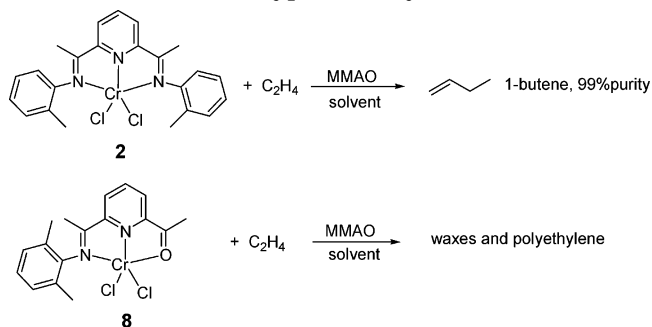


**Figure 2.** Branching increases as the ratio of comonomer to ethylene increases: (A) wax produced at 27 bar ethylene (Table 1, entry 13); (B) wax produced at 1.0 bar ethylene (entry 10); (C) wax produced with 20% 1-hexene comonomer present (entry 16). See Table 1 for details.

### Scheme 2. Comparison of Products for Type 1 (top) and Type 2 Catalysts



containing system produces much higher molecular weight oligomers than the pyridine bisimine catalyst is somewhat counterintuitive. Entries 1–6 suggest that ligand steric bulk plays a key role in determining product molecular weight. Thus, one might have predicted that the inherently bulkier Type 1 catalysts would make higher oligomers than Type 2. However, the trend is surprisingly reversed, indicating that simple steric arguments alone cannot be used to rationalize the relative product distributions of the two catalyst systems. Close inspection of Scheme 2 shows that complex **2** (Type 1) and complex **8** (Type 2) possess the same total number of *ortho* methyl groups, but the Type 2 ketone-containing catalyst has both methyl groups on the same ring and makes a much higher molecular weight product. This observation seems to indicate that the presence of two *ortho* substituents on a single aryl ring results in polymer or heavy oligomer formation, regardless of the presence of a second imino–aryl moiety. This same effect is observed for the isopropyl-substituted systems (entry 4 vs entry 11) and for catalysts run at elevated pressure (entry 9 vs entries 13 and 14).

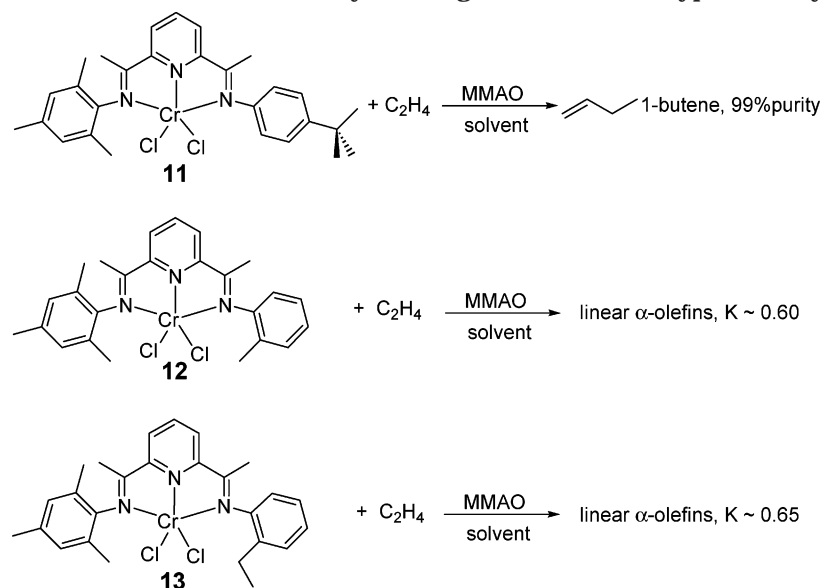
To test whether the location of the *ortho* methyl groups—i.e., both on the same aryl ring or one on each ring—was the primary factor in determining product molecular weight, a new Type 1 complex with an asymmetric NNN donor set was synthesized. This complex **11**, shown in Scheme 3, may be viewed as a hybrid between the two species shown in Scheme 2. Although this new system possesses the same location of the *ortho* methyl groups as the Type 2 catalyst, it has

the base ligand of the Type 1 complexes. Activation of this new catalyst under 1.0 bar of ethylene results in almost exclusive and rapid dimerization of ethylene to 1-butene, a clear indicator of ‘Type 1’ behavior (Table 1, entry 17). This experiment demonstrates that steric arguments made for the Type 1 systems are not predictive of behavior for the Type 2 catalysts and vice versa.

The propensity of Type 1 catalysts bearing two total *ortho* methyl groups to produce butene (entries 2 and 17), along with the tendency of the system with four *ortho* methyl groups to make waxes (entry 6), suggested that an intermediate degree of steric bulk might produce catalysts for making  $\alpha$ -olefins with a more commercially typical Schulz–Flory constant (0.6–0.8). With that goal in mind, asymmetric precatalysts **12** and **13** in Scheme 3 were synthesized and used to oligomerize ethylene. As shown by Scheme 3, catalysts bearing three total *ortho* alkyl groups produce linear  $\alpha$ -olefins with high productivity and selectivity and with product molecular weights that are between the molecular weights made by the less substituted and more highly substituted analogues. Entry 18 (complex **12**) provides more details about the oligomerization reaction, and entry 19 contains the results from using the slightly more bulky ethyl-substituted **13**. Note, the products made in entry 19 are slightly heavier (demonstrated by a slightly larger *K* value) than those made in entry 18, indicating that for some Type 1 catalysts rational ligand modifications can lead to predictable product properties.

**Discussion of Polymer Molecular Weight Data.** Regardless of the product distribution, all of the catalysts in this report, whether derived from the chromium(II) or the chromium(III) source, made significant quantities of polyethylene coproduct. In the cases of ethylene dimerization catalyzed by the Type 1 systems, this contrast was stark; for the catalysts that made higher oligomers, the distinction was less noticeable. Gel-permeation chromatography (GPC) was used to analyze the polymers made in experiments 5–19 in Table 1. Upon examination of the GPC data, many of the traces showed bimodal or even polymodal behavior. For pyridine bisimine iron catalysts, it is known that the MAO:metal ratio impacts product molecular weight, with higher MAO loadings yielding lower molecular weight product via chain transfer to aluminum.<sup>13d</sup> We

## Scheme 3. Steric Effects on Ethylene Oligomerization for Type 1 Catalysts

Table 2. Polymerization Data for **7'** with Varying Al:Cr Ratios

entry	Al:Cr mol ratio	productivity (g of PE/g of Cr complex)	$M_w$	$M_w/M_n$
20	100	730	55 000	7.9
21	200	830	37 700	9.0
22	400	1080	32 200	10.1
23	800	1450	33 700	12.5

<sup>a</sup> Polymerizations were performed under the following conditions: 10  $\mu$ mol of chromium complex in 100 mL of toluene, 40 °C, 1.3 bar, 1 h.

were curious to see how the polymers made by the chromium catalysts would be affected by the cocatalyst level. We carried out a separate study examining the effect of Al:Cr ratio on catalyst productivity and polymer molecular weight for the 2,5-di-*tert*-butyl-substituted complex **7'**. The data are contained in Table 2. For this study, complex **7'** is especially useful since it produces predominantly moderate molecular weight polyethylene that is readily analyzed by GPC. As expected, increasing the Al:Cr ratio from 100 to 800 results in a gradual increase in catalyst productivity. It is also clear from the  $M_w$  and  $M_w/M_n$  data in Table 2 that lower molecular weight product is formed at higher Al:Cr ratios. The GPC traces, shown in Figure 3, are even more instructive as they distinctly show the dramatic increase in low molecular weight material (peak centered at about MW = 1000) as the Al:Cr ratio increases. The GPC traces are reminiscent of those reported for iron(II)-based catalysts and are consistent with chain transfer to aluminum as a likely route for the formation of low-molecular-weight polymers. In addition, <sup>13</sup>C NMR data (not shown) of the polymers produced in entries 20–23 indicate that substantial quantities of olefinic products are formed for Al:Cr ratios up to 200 but that increasing amounts of saturated products are formed at Al:Cr > 200, again consistent with chain transfer to aluminum as a likely termination mechanism. Changing the Al:Cr ratio clearly explains one way to generate bimodal polymers, but polymodal behavior likely indicates that more than one catalyst active species is present. The possible nature of these species is discussed later in this report.

The molecular weights reported in Table 1 are the peak molecular weights of the largest peak in the GPC trace. Since all of the catalysts that produce mainly low-molecular-weight coproducts, the peak values reported in Table 1 are more useful than the  $M_n$  and  $M_w$  values for the purposes of the following discussion. However, the  $M_n$  and  $M_w$  values, along with the GPC traces, are included in the Supporting Information.

As found for the iron and cobalt pyridine bisimine catalysts, the molecular weights of polymers produced by chromium pyridine bisimine compounds are largely dependent on the steric bulk at the *ortho* positions of the aryl rings. The effect of ligand sterics on the product distribution for the NNN chromium complexes was discussed earlier, but this effect is also seen for the NNO catalysts. For example, comparing complexes **8** and **9** (entries 10 and 11), the methyl-substituted catalyst makes lower molecular weight polyethylene than the isopropyl-substituted system (peak MW's 34 000 and 68 200, respectively), and both produce lower molecular weight polymer than *tert*-butyl derivative **10** (peak MW = 103 000). Also, the data clearly indicate that the NNO catalysts (entries 10–12) make higher molecular weight polymers than the NNN catalysts. In fact, according to the GPC numbers, the NNN catalysts produced primarily wax products, with peak molecular weights of < 1000 (entries 5–8). Complex **7** was the exception to this trend, producing a polymer with a peak MW of 11 000 (entry 8). Due to the peculiar bimodal and polymodal behavior of these catalysts, more study is needed to more fully assess these molecular weight trends.

**Crystallographic Studies.** To better characterize the molecular structures of the chromium(II) and chromium(III) pyridine bisimine precatalysts, we examined complexes **5'**, **6'**, and **6** using X-ray crystallography. Complex **5'**, containing the 2-*tert*-butyl-substituted ligand, is of special interest since it displays low activity compared to other 2-alkyl-substituted complexes, as well as compared to 2,6-disubstituted derivatives such as **6'**. Furthermore, the structure of chromium(II) complex **6** allows us to directly compare chromium(II) and chromium(III) complexes with the same ligand set. Unfortunately, despite repeated attempts, we were unable to

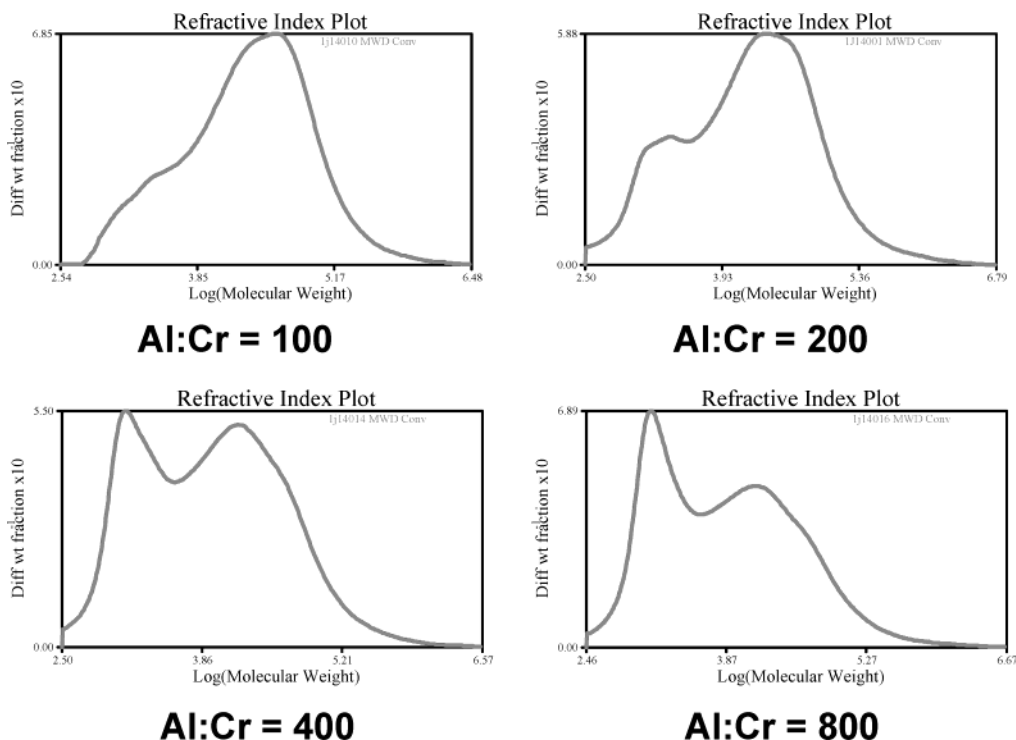


**Figure 3.** GPC traces for polymer produced using 7' with varying Al:Cr ratios.

**Table 3. Summary of X-ray Crystallographic Data for Chromium Complexes 5', 6', and 6<sup>a</sup>**

complex	5'	6'	6
empirical formula	C <sub>32</sub> H <sub>39.5</sub> Cl <sub>3</sub> CrN <sub>4.5</sub>	C <sub>25</sub> H <sub>27</sub> Cl <sub>3</sub> CrN <sub>3</sub>	C <sub>25</sub> H <sub>27</sub> Cl <sub>2</sub> CrN <sub>3</sub>
fw	645.52	527.85	492.40
cryst syst	triclinic	monoclinic	monoclinic
space group	<i>P</i> 1	<i>P</i> 2 <sub>1</sub> / <i>c</i>	<i>P</i> 2 <sub>1</sub> / <i>c</i>
<i>a</i> (Å)	9.834(3)	11.148(5)	12.626(1)
<i>b</i> (Å)	12.942(3)	15.492(3)	11.740(2)
<i>c</i> (Å)	15.375(3)	14.393(4)	16.790(2)
$\alpha$ (°)	112.99(4)	90	90
$\beta$ (°)	96.97(3)	92.59(3)	98.362(6)
$\gamma$ (°)	105.19(3)	90	90
<i>V</i> (Å <sup>3</sup> )	1682.4(7)	2483.2(14)	2462.3(5)
<i>Z</i>	2	4	4
<i>d</i> <sub>calc</sub> (Mg·m <sup>-3</sup> )	1.271	1.412	1.328
cryst size (mm)	0.40 × 0.40 × 0.10	0.35 × 0.32 × 0.06	0.38 × 0.20 × 0.12
abs. coeff. (mm <sup>-1</sup> )	0.606	0.802	0.698
2 $\theta$ max (°)	50.08	49.98	50.08
transmission range	1.0–0.5305	1.0–0.8879	1.0–0.9128
no. of reflns collected	6311	4589	4554
no. of indep reflns	5936	4353	4345
no. of obsd reflections	3102	3038	2678
no. of variables	377	289	280
<i>R</i> 1 ( <i>wR</i> 2) <sup>b</sup> [ <i>I</i> > 2 $\sigma$ ( <i>I</i> )]	0.0808 (0.1840)	0.0397 (0.0985)	0.0792 (0.1447)
goodness-of-fit ( <i>F</i> <sup>2</sup> )	1.003	1.027	1.029
diff. peaks (e <sup>-</sup> ·Å <sup>-3</sup> )	1.121, -0.687	0.366, -0.270	0.343, -0.331

<sup>a</sup> See Experimental Section for additional data collection, reduction, and structure solution and refinement details. <sup>b</sup>  $R1 = \sum |F_o| - |F_c| / \sum |F_o|$ ;  $wR2 = [\sum (w(F_o^2 - F_c^2)^2)]^{1/2}$ , where  $w = 1/\sigma^2(F_o^2) + (aP)^2 + b$ .

obtain suitable single crystals of Type 2 (NNO) complexes. A summary of crystal data collection parameters for 5', 6', and 6 is given in Table 3.

*Structures of {2,6-Bis[1-((2,6-dimethylphenyl)imino)ethyl]pyridine}CrCl<sub>3</sub> (6') and {2,6-Bis[1-((2-tert-butylphenyl)imino)ethyl]pyridine}CrCl<sub>3</sub>·1.5CH<sub>3</sub>CN (5').* Crystals of 6' and 5' suitable for X-ray structure determination were obtained by slow evaporation of acetonitrile solutions of the respective compounds. The molecular structures are shown in Figure 4, and selected distances and angles are given in Table 4. The structures of 6' and 5' are similar to that of {2,6-bis[1-((2,6-diisopropylphenyl)imino)ethyl]pyridine}CrCl<sub>3</sub> (14'), re-

ported separately by Gambarotta<sup>19a</sup> and Esteruelas.<sup>11a</sup> Similarities include the fact that the Cr–N(pyridyl) distances are shorter (0.13–0.16 Å) than the Cr–N(imino) bonds and the equatorial Cr–Cl bond (opposite the pyridyl nitrogen) is the shortest of the three Cr–Cl distances. Also, as expected, the phenyl ring planes in 6' and 5' are oriented nearly perpendicular to the plane of the pyridine bisimine ligand (dihedral angles ranging from 67.5° to 94.6°) to minimize steric interactions between the aryl substituents and the remainder of the complex.

In addition, 6', like 14', possesses one long axial Cr–Cl bond. For 6', the long Cr–Cl bond (Cr–Cl(3) =

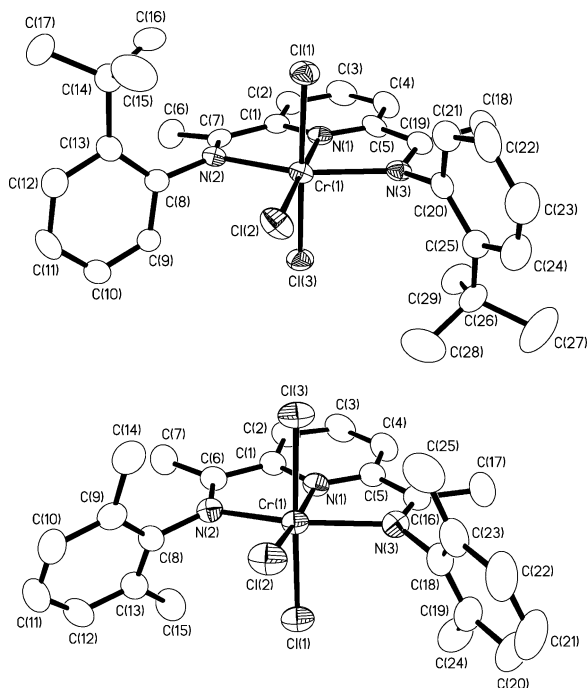


**Figure 4.** Thermal ellipsoid representation (35% probability boundaries) of the X-ray crystal structures of **5'** (top) and **6'** (bottom). Hydrogen atoms are omitted for clarity.

**Table 4. Selected Distances (Å) and Angles (deg) for Structurally Characterized Complexes<sup>a</sup>**

complex <b>6'</b>			
Cr(1)–N(1)	1.993(3)	Cr(1)–Cl(2)	2.2695(10)
Cr(1)–N(2)	2.123(3)	Cr(1)–Cl(3)	2.3513(13)
Cr(1)–N(3)	2.140(3)	N(2)–C(6)	1.291(4)
Cr(1)–Cl(1)	2.2996(13)	N(3)–C(16)	1.297(4)
N(1)–Cr(1)–N(2)	75.75(11)	N(2)–Cr(1)–Cl(3)	98.57(7)
N(1)–Cr(1)–N(3)	77.24(11)	N(3)–Cr(1)–Cl(1)	87.69(8)
N(2)–Cr(1)–N(3)	153.36(10)	N(3)–Cr(1)–Cl(2)	103.10(8)
N(1)–Cr(1)–Cl(1)	94.45(8)	N(3)–Cr(1)–Cl(3)	90.50(8)
N(1)–Cr(1)–Cl(2)	173.25(8)	Cl(1)–Cr(1)–Cl(2)	92.30(4)
N(1)–Cr(1)–Cl(3)	81.43(8)	Cl(1)–Cr(1)–Cl(3)	175.78(4)
N(2)–Cr(1)–Cl(1)	88.68(8)	Cl(2)–Cr(1)–Cl(3)	91.82(4)
N(2)–Cr(1)–Cl(2)	103.41(8)		
complex <b>5'</b>			
Cr(1)–N(1)	1.981(5)	Cr(1)–Cl(2)	2.270(2)
Cr(1)–N(2)	2.141(6)	Cr(1)–Cl(3)	2.319(3)
Cr(1)–N(3)	2.127(6)	N(2)–C(7)	1.284(8)
Cr(1)–Cl(1)	2.308(3)	N(3)–C(19)	1.288(8)
N(1)–Cr(1)–N(2)	77.9(2)	N(2)–Cr(1)–Cl(3)	86.32(15)
N(1)–Cr(1)–N(3)	76.9(2)	N(3)–Cr(1)–Cl(1)	87.04(15)
N(2)–Cr(1)–N(3)	154.81(19)	N(3)–Cr(1)–Cl(2)	102.85(15)
N(1)–Cr(1)–Cl(1)	87.16(16)	N(3)–Cr(1)–Cl(3)	91.57(16)
N(1)–Cr(1)–Cl(2)	178.28(17)	Cl(1)–Cr(1)–Cl(2)	94.54(9)
N(1)–Cr(1)–Cl(3)	85.38(16)	Cl(1)–Cr(1)–Cl(3)	172.54(8)
N(2)–Cr(1)–Cl(1)	91.82(15)	Cl(2)–Cr(1)–Cl(3)	92.92(9)
N(2)–Cr(1)–Cl(2)	102.33(14)		
complex <b>6</b>			
Cr(1)–N(1)	1.993(5)	Cr(1)–Cl(2)	2.406(2)
Cr(1)–N(2)	2.128(5)	N(2)–C(6)	1.286(7)
Cr(1)–N(3)	2.107(5)	N(3)–C(17)	1.294(7)
Cr(1)–Cl(1)	2.3215(18)		
N(1)–Cr(1)–N(2)	76.11(19)	N(2)–Cr(1)–Cl(1)	102.14(14)
N(1)–Cr(1)–N(3)	75.6(2)	N(2)–Cr(1)–Cl(2)	98.03(14)
N(2)–Cr(1)–N(3)	148.5(2)	N(3)–Cr(1)–Cl(1)	98.09(15)
N(1)–Cr(1)–Cl(1)	155.92(15)	N(3)–Cr(1)–Cl(2)	101.99(15)
N(1)–Cr(1)–Cl(2)	104.12(15)	Cl(1)–Cr(1)–Cl(2)	99.92(7)

<sup>a</sup> Estimated standard deviations are indicated in parentheses.

2.3513(13) Å) coincides with a subtle canting of the pyridine bisimine ligand toward Cl(3), which manifests itself in an acute N(1)–Cr–Cl(3) angle of 81.43(8)°. While this canting accommodates the methyl substitu-

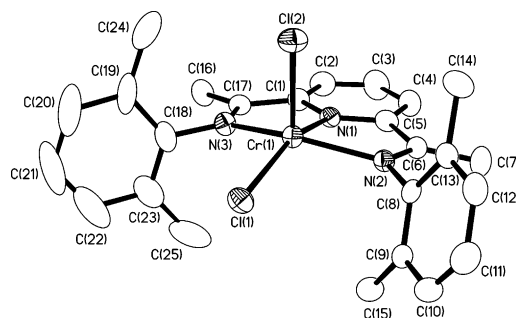


**Figure 5.** Thermal ellipsoid representation (35% probability boundaries) of the X-ray crystal structure of **6**. Hydrogen atoms are omitted for clarity.

ents that are directed toward Cl(1), it simultaneously increases the steric interactions between the remaining two methyl substituents and Cl(3), lengthening the Cr–Cl(3) bond. The structure of **14'** reported by Esteruelas also displays an acute Cl–Cr–N(pyridyl) angle (82.27(8)°) with attendant tilting of the pyridine bisimine ligand toward the long Cr–Cl bond.<sup>11a</sup> While this distortion is notable, at this time it is unclear whether the distortion is retained in solution or whether it persists in the activated catalyst.

In contrast to **6'** and **14'**, complex **5'** displays nearly equivalent N(pyridyl)–Cr–Cl angles (N(1)–Cr–Cl(1) = 87.16(16)° and N(1)–Cr–Cl(3) = 85.38(16)°) and the axial Cr–Cl bond lengths are also similar (2.308(3) Å and 2.319(3) Å). Apparently, complex **5'** accommodates the *2-tert*-butyl substituents without significant tilting of the pyridine bisimine ligand, in part by positioning the *tert*-butyl groups in an anti arrangement. We should note that the anti arrangement appears to provide a reasonably accessible metal center. Thus, the reasons for the low activity of **5'** relative to other 2-substituted derivatives are not readily apparent from the solid-state structure.

*Structure of {2,6-Bis[1-((2,6-dimethylphenyl)imino)ethyl]pyridine}CrCl<sub>2</sub> (**6**).* Slow cooling of a saturated CH<sub>2</sub>Cl<sub>2</sub> solution deposited single crystals of **6**. The structure is shown in Figure 5, and selected distances and angles are included in Table 4. The pseudo-square-pyramidal structure of **6** is reminiscent of certain 5-coordinate iron(II) and cobalt(II) pyridine bisimine derivatives reported by Gibson and Brookhart.<sup>13,14</sup> For **6**, the basal plane consists of the three nitrogen atoms from the pyridine bisimine ligand and one equatorial chloride, with the remaining chloride occupying the apical position. In this geometry, the chromium atom is raised 0.40 Å above the basal plane. In the iron(II) and cobalt(II) pyridine bisimine derivatives, the metal–Cl(apical) bonds are longer (0.04–0.06 Å) than the corresponding equatorial M–Cl distances. The same trend is observed for **6**, with the apical Cr–Cl(2) bond (2.406(2) Å) being 0.08 Å longer than its equatorial counterpart (2.3215(18) Å). As expected, given the larger atomic radius of chromium(II), the Cr–Cl bonds in **6** are longer than the average Cr–Cl distances in the chromium(III) derivatives **6'** and **5'**. However, the Cr–N(pyridyl) and Cr–N(imino) distances in **6** are similar to, if not slightly shorter than, those in **6'** and **5'**. The near equivalence of the Cr–N distances in the two oxidation states is presumably due to the lower coordination number in **6** relative to **6'** and **5'**. Finally, the C–N(imino) distances in **6** (1.286(7) and 1.294(7) Å) indicate that the imino groups have retained their double-bond character and that the ligand binds as a

neutral pyridine bisimine to the chromium(II) center—there is no structural evidence for significant electron delocalization from the reduced metal center to the ligand.

**Nature of the Catalyst Active Species.** The ability to draw a loose connection between the ligand sterics and the product molecular weights within each catalyst family, along with the *inability* to extend the steric connection between the two catalyst types, suggests that the Type 1 (NNN) and Type 2 (NNO) catalysts differ from each other in charge, chain growth mechanism, oxidation state, and/or some other feature. An examination of the literature shows that the tridentate ligand/metal combination can lead to wide variations in the electronics of the formed complexes; in that regard, it is not too surprising that the Type 1 catalyst sterics are not predictive for the Type 2 systems and vice versa.

A number of recent studies on pyridine bisimine complexes have reported a wide variety of organometallic species, covering a wide range of oxidations states, responses to alkylating agents, and catalyst initiation mechanisms. For example, in the case of pyridine bisimine vanadium systems, ligand alkylation by the cocatalyst causes the formation of an anionic ligand.<sup>20</sup> Moving to the later transition metals, a neutral tridentate manganese(I) complex and an anionic manganese(II) complex have been isolated and characterized.<sup>19b</sup> Neither of these species nor the manganese(II) dichloride precursor are initiators or precatalysts for olefin polymerization. For the tridentate iron analogues, recent studies using trimethylaluminum as the cocatalyst for ethylene polymerization reactions led the authors to propose a neutral iron(II) active species.<sup>21</sup> For the tridentate cobalt catalysts, two very recent studies suggest that polymerization might be initiated by a cationic cobalt(I) complex, which may undergo propagation via a cobalt(III) species.<sup>22</sup> With ruthenium, a cationic ruthenium(II) alkyl olefin complex has been isolated, but this species is not active for polymerization.<sup>23</sup> For rhodium, yet another type of complex, a dicationic rhodium(III) alkyl olefin species, has been identified. This rhodium complex is also not active for ethylene polymerization.<sup>23</sup> None of these basic structures may at this point be ruled out for these new chromium catalysts. Furthermore, we should note that the ketone group in Type 2 systems may be especially susceptible to attack by aluminum alkyls, perhaps generating an in situ alkoxide or Lewis acid–base adduct.

Despite difficulties in preparing analytically pure chromium(II) complexes, the chromium(II) and chromium(III) catalysts exhibit equal activities and make the same products upon activation. These results certainly imply that identical active species are generated in the presence of MAO, but more evidence was sought to justify this assertion.<sup>24</sup> A UV–vis study<sup>25</sup> was chosen, in which the chromium(II) and chromium(III) Type 1 complexes **6** and **6'** were analyzed before and after the addition of MAO (10 wt % in toluene). As Figure 6 indicates, the addition of MAO generates the same UV spectrum for each complex, a result that agrees with their nearly identical catalytic activities. To further support the argument of identical catalyst active species, GPC data was obtained for the polyethylenes made by the activated complexes **6**, **6'**, **14**, and **14'** under identical polymerization conditions. As shown in Table 5 and Figure 7, the polymers made by **6** and **6'** are very

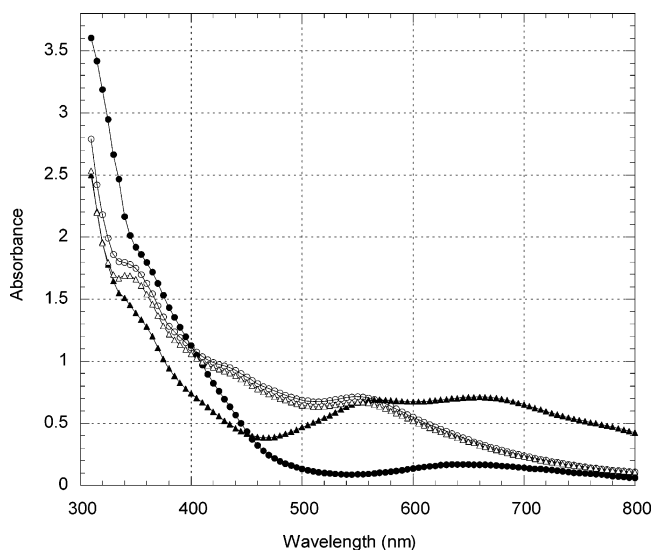


**Figure 6.** UV–vis spectra of **6'** (●), **6'** + 200 equiv of MAO (○), **6** (▲), **6** + 200 equiv of MAO (△). Samples are 5 mM in  $\text{CH}_2\text{Cl}_2$ . Spectra of samples with added MAO were acquired within 15 min after MAO addition.

similar as are the polymers made by **14** and **14'**. This evidence further suggests the identical nature of the chromium(II) and chromium(III) active species.

In conclusion, a highly active family of chromium catalysts for the dimerization and oligomerization of ethylene has been introduced. Although these are not the first chromium systems known to dimerize ethylene,<sup>26</sup> the high purity of the 1-butene and the high activity of the catalysts are remarkable. In addition to the butene production, the catalysts also make highly linear  $\alpha$ -olefin waxes and readily incorporate comonomer to make branched waxes. As shown in Table 1, these catalysts are quite robust, exhibiting high activity up to at least 100 °C. Finally, the ligand substituent effects on the product composition are profound and for the most part predictable within each catalyst type (NNN and NNO complexes). Further studies will focus on optimizing the oligomerization reaction conditions, gaining a better understanding of the relationship between catalyst sterics and activity, studying the copolymerization reactions in more detail, and gaining more information about the nature of the catalytically active species.

## Experimental Section

**Materials and Methods.** Anhydrous tetrahydrofuran, toluene, heptane, and cyclohexane were purchased from Aldrich and stored over molecular sieves. Acetonitrile was distilled from calcium hydride and stored over molecular sieves. 1-Hexene was obtained as a commercial grade of Chevron Phillips' Normal Alpha Olefins (NAO's), degassed, and dried over 4A molecular sieves. MMAO-3A (Al 7% by weight) was purchased from Akzo Nobel. MAO (10 wt %) in toluene was provided by Albemarle. 2,6-Diacetylpyridine, chromium(II) chloride, tris-(tetrahydrofuran)chromium(III) chloride, and all substituted anilines were purchased from Aldrich and used without further purification. NMR spectra were obtained using a Varian Unity Plus 300 MHz Spectrometer. Elemental analyses were performed by Atlantic Microlabs of Norcross, GA. Gel-permeation chromatography (GPC) data for Figure 3 were obtained on a Waters 150 °C GPC operating at 140 °C using 1,2,4-trichlorobenzene as solvent. GPC data for Table 1 were obtained with a PL 210 SEC high-temperature chromatography unit (Polymer Laboratories) equipped with three PLgel 10  $\mu\text{m}$  Mixed A columns (Polymer Laboratories). A refractive index detector

Table 5. Comparative Polymerization Data for Chromium(II) and Chromium(III) Complexes<sup>a</sup>

entry	catalyst system <sup>b</sup>	substituent R <sub>n</sub>	substituent R' <sub>n</sub>	productivity (g of PE/g of Cr complex)	M <sub>w</sub>	M <sub>w</sub> /M <sub>n</sub>
24	<b>6</b> , MAO	2,6-Me <sub>2</sub>	2,6-Me <sub>2</sub>	410	1300	1.6
25	<b>6'</b> , MAO	2,6-Me <sub>2</sub>	2,6-Me <sub>2</sub>	430	1200	1.3
26	<b>14</b> , MAO	2,6- <sup>i</sup> Pr <sub>2</sub>	2,6- <sup>i</sup> Pr <sub>2</sub>	580	21 600	4.2
27	<b>14'</b> , MAO	2,6- <sup>i</sup> Pr <sub>2</sub>	2,6- <sup>i</sup> Pr <sub>2</sub>	420	17 300	5.2

<sup>a</sup> Polymerizations were performed under the following conditions: 10 μmol of chromium complex in 100 mL of toluene, Al:Cr = 200, 40 °C, 1.3 bar, 1 h. <sup>b</sup> Commercial MAO from Albemarle (10 wt % MAO in toluene) was used in these studies.

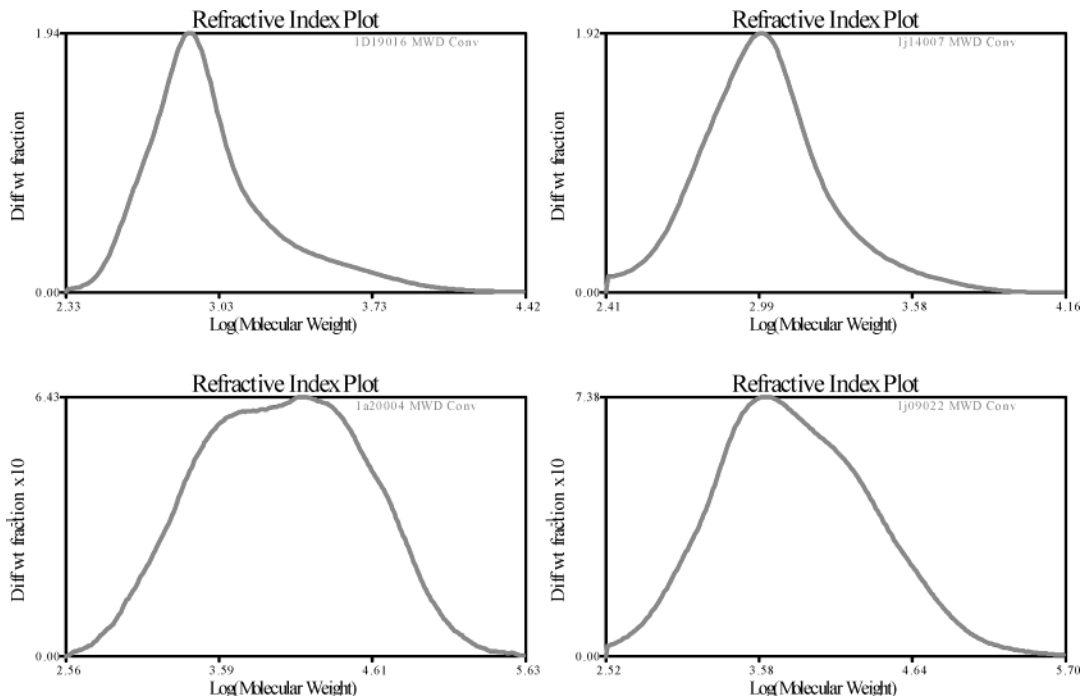


**Figure 7.** Gel permeation chromatography traces of polymer produced from chromium(II) and chromium(III) complexes under low-pressure polymerization conditions. The chromium complexes used are identified as follows: **6** (upper left), **6'** (upper right), **14** (lower left), **14'** (lower right). Polymerization conditions: 40 °C, 1.3 bar, Al:Cr = 200, 10 μmol of compound in 100 mL of toluene, 1 h.

was used for molecular weight determinations. Samples (1 mg/mL) were chromatographed at 1 mL/min using 1,2,4-trichlorobenzene as the mobile phase. Columns were calibrated using a broad molecular weight, PE standard. <sup>13</sup>C NMR measurements on polymer samples were conducted at 120 °C in 1,1,2,2-tetrachloroethane using a Bruker ACE 300 spectrometer. Samples for IR were dispersed in KBr, and spectra were recorded on a Nicolet 5DXC spectrometer with a diffuse reflectance (DRIFTS) attachment. A Hewlett-Packard 6890 Series GC System with an HP-5 50m column with a 0.2 mm i.d., an initial oven temperature of 35 °C, and a ramp rate of 2.4 °C/min. was used for analysis of the light oligomers. An HP 5890 GC System with a Chrompak WCOT Ulti-Metal 10m column with a 0.5 mm i.d., an initial oven temperature of 100 °C, a ramp rate of 8.0 °C/min, and a final temperature of 400 °C was used for analysis of the waxes. Helium was the carrier gas for both instruments, and FID detection was used. ChemStation from Agilent Technologies was used to analyze the collected data. MALDI mass spectrometry data were obtained using a BiFlexIII MALDI mass spectrometer. ESI mass spectrometry data were obtained using Micromass AutoSpec Ultima Magnetic sector mass spectrometer.

**Synthesis of Ligands.** Syntheses of the tridentate ligands used to prepare complexes of both Type 1 and Type 2 have been previously reported.<sup>13,14</sup> Modest adaptations of those methods were used to prepare the ligands used herein. For new ligands, complete synthetic and characterization details are given. For previously reported ligands, only significant synthetic modifications are presented.

**6-[1-((2,6-Dimethylphenyl)imino)ethyl]-2-acetylpyridine (Type 2; 2,6-Me<sub>2</sub>).** A 3.0 g (18.4 mmol) amount of 2,6-

diacetylpyridine and 2.3 mL (18.7 mmol) of 2,6-dimethyl aniline were stirred together in a flask with 20 mL of anhydrous methanol. Several drops of glacial acetic acid were added, and the reaction was heated with stirring for 3 days at 55 °C. The reaction flask was then placed in a freezer at -20 °C, resulting in the formation of yellow, needlelike crystals. These crystals were removed by filtration and washed with cold methanol (yield = 1.15 g, 24%). <sup>1</sup>H NMR (CDCl<sub>3</sub>) δ 2.12 (s, 6H, aryl CH<sub>3</sub>), 2.26 (s, 3H, acetyl CH<sub>3</sub>), 2.86 (s, 3H, imino CH<sub>3</sub>), 7.01 (t, 1H, aryl CH), 7.17 (d, 2H, aryl CH), 8.00 (dd, 1H, pyr. CH), 8.18 (d, 1H, pyr. CH), 8.64 (d, 1H, pyr. CH).

**6-[1-((2,4,6-Trimethylphenyl)imino)ethyl]-2-acetylpyridine (Type 2; 2,4,6-Me<sub>3</sub>, Mes NNO).** This compound may be prepared according to the method reported in the literature.<sup>14e</sup>

**2-[1-((2,4,6-Trimethylphenyl)imino)ethyl]-6-[1-((4-tert-butylphenyl)imino)ethyl]pyridine (Type 1; 2,4,6-Me<sub>3</sub>; 4-tBu).** A 5.00 g (18 mmol) amount of the monoimine (Mes NNO) was dissolved with 4.3 mL (27 mmol) of 4-tert-butylaniline in ethanol (50 mL). Five drops of acetic acid were added, and the reaction was heated with stirring at 60 °C for 18 h. The heating was discontinued, and the reaction was allowed to sit at room temperature. After 2 days, 4.44 g (61% yield) of needlelike crystals was isolated, washed with ethanol, and identified by <sup>1</sup>H NMR as the pure desired product. This compound has been previously reported.<sup>14e</sup>

**2-[1-((2,4,6-Trimethylphenyl)imino)ethyl]-6-[1-((2-methylphenyl)imino)ethyl]pyridine (Type 1; 2,4,6-Me<sub>3</sub>; 2-Me).** A 1.0 g (3.6 mmol) amount of the monoimine (Mes NNO) was dissolved with 0.57 g (5.3 mmol) of *o*-toluidine in methanol (10 mL). Three drops of acetic acid were added, and

the reaction was heated with stirring at 60 °C for 16 h. The reaction was allowed to cool, then was placed in a freezer at 0 °C, resulting in the formation and collection of 262 mg (20%) of needlelike crystals that were identified as pure by NMR. <sup>1</sup>H NMR (CDCl<sub>3</sub>) δ 1.87 (s, 6H, mes. *o*-CH<sub>3</sub>), 2.11 (s, 3H, *o*-tol. CH<sub>3</sub>), 2.22 (s, 3H, mes. *p*-CH<sub>3</sub>), 2.28 (s, 3H, imino CH<sub>3</sub>), 2.34 (s, 3H, imino CH<sub>3</sub>), 6.63 (d, 1H, tol. ring), 6.84 (s, 2H, mes. ring), 7.02 (m, 1H, tol. ring), 7.20 (m, 2H, tol. ring), 7.81 (dd, 1H, py. H<sub>p</sub>), 8.41 (d, 1H, py. H<sub>m</sub>), 8.43 (d, 1H, py. H<sub>m</sub>). <sup>13</sup>C NMR (CDCl<sub>3</sub>) δ 16.0 (2), 17.5 (3), 20.5 (1), 118.1 (1), 122.3 (2), 123.4 (1), 124.9 (2), 126.2 (1), 127.0 (1), 128.4 (2), 130.3 (1), 132.1 (1), 136.6 (1), 145.8 (1), 150.1 (1), 155.2 (1), 155.4 (1), 166.7 (1), 167.8 (1); 25 chemically different carbons, but several show chemical shift equivalence.

**2-[1-{(2,4,6-Trimethylphenyl)imino}ethyl]-6-[1-{2-ethylphenyl}imino]ethyl]pyridine (Type 1; 2,4,6-Me<sub>3</sub>; 2-Et).** A 1.0 g (3.6 mmol) amount of the monoimine (Mes NNO) was dissolved with 1.30 g (10.7 mmol) of *o*-toluidine in methanol (10 mL). Three drops of acetic acid were added, and the reaction was heated with stirring at 60 °C for 16 h. The reaction was allowed to cool, then was placed in a freezer at 0 °C, resulting in the formation and collection of 247 mg (20%) of needlelike crystals that were identified as pure by NMR. <sup>1</sup>H NMR (CDCl<sub>3</sub>) δ 1.20 (t, 3H, CH<sub>3</sub> on ethyl), 1.98 (s, 6H, mes. *o*-CH<sub>3</sub>), 2.23 (s, 3H), 2.29 (s, 3H), 2.34 (q, 2H, CH<sub>2</sub> on ethyl), 2.35 (s, 3H), 6.62 (d, 1H, tol. ring), 6.87 (s, 2H, mes. ring), 7.07 (t, 1H, tol. ring), 7.24 (m, 2H, tol. ring), 7.88 (t, 1H, py. H<sub>p</sub>), 8.41 (d, 1H, py. H<sub>m</sub>), 8.43 (d, 1H, py. H<sub>m</sub>). <sup>13</sup>C NMR (CDCl<sub>3</sub>) δ 14.5 (1), 22.8 (1), 27.1 (1), 29.2 (1), 29.7 (2), 32.0 (1), 117.8 (1), 121.9 (1), 122.1 (1), 123.7 (1), 125.1 (2), 126.3 (1), 128.3 (2), 128.6 (1), 132.1 (1), 133.5 (1), 136.8 (1), 146.4 (1), 149.2 (1), 155.2 (1), 155.4 (1), 166.3 (1), 167.8 (1); 26 chemically different carbons, but several show chemical shift equivalence.

**Synthesis of Chromium Precatalyst Complexes.** Chromium complexes of both Type 1 and Type 2 were prepared using slight modifications of the reported procedure for preparation of analogous iron and cobalt complexes.<sup>13</sup> In general, a slight excess of the ligand (~1.1equiv) was stirred with the chromium source in hot THF for 1 day, followed by precipitation with pentane, filtration under inert atmosphere, and washing with ether and pentane. Yields of about 70% or higher could be obtained for all complexes in this manner (see Table 6). However, elemental analyses for the chromium(II) precursors indicated substantial deviation from the calculated values for many of the complexes. Bulkier ligands typically resulted in poorer CHN analysis values (3% or more low for carbon). Satisfactory elemental analyses for the chromium(III) complexes are reported in Table 6.

**Oligomerization of Ethylene.** In an oxygen- and moisture-free environment, the chromium precatalyst, solvent, comonomer (if any), and a stir bar were added to a flask. The flask was transferred to a Schlenk manifold and placed under a continuous ethylene purge. The flask contents were stirred rapidly for several minutes to saturate the solvent with ethylene and to break apart any small chunks of precatalyst. MMAO-3A was added via syringe. Optionally, a cooling bath was used to maintain the desired reaction temperature. For reactions in which light olefins were the primary product, the ethylene was continuously purged through the reaction flask. For the wax-producing reactions, the ethylene was fed "on demand".

For reactions at elevated pressure, a 500 mL Zipperclave reactor from Autoclave Engineers was used. The catalyst was dissolved in a small amount of dichloromethane in an NMR tube, which was then sealed and bound to the stirrer shaft of the clean, dry reactor. The reactor was evacuated, then charged with the solvent and the alumoxane cocatalyst. The desired pressure of ethylene was introduced, and the reactor stirrer was started, resulting in breakage of the NMR tube and catalyst activation. Ethylene was fed "on demand" using a TESCOM regulator, and the reactor temperature was maintained by internal cooling. An external heating mantle was used for reactions that were not sufficiently exothermic to reach the desired temperature. All of the reactions were

Table 6. Characterization of Chromium(II) Complexes

com- plex type <sup>a</sup>	cat. type <sup>a</sup>	subst. <sup>b</sup> R <sub>n</sub>	subst. <sup>b</sup> R' <sub>n</sub>	% yield <sup>c</sup>	formula	calcd (%)			found (%)			IR (KBr, cm <sup>-1</sup> )	mass spec. <sup>e</sup>
						C	H	N	C	H	N		
1	1	2-H	2-H	72	C <sub>21</sub> H <sub>19</sub> N <sub>3</sub> Cl <sub>3</sub> Cr	53.47	4.06	8.91	52.57	4.40	8.73	2917, 2852, 1581, 1487, 1368, 1274, 1238, 841, 780, 698	(ES <sup>+</sup> ): m/z 467 [M - Cl + CH <sub>3</sub> OH] <sup>+</sup> ; (ES <sup>-</sup> ): m/z 435 [M - Cl] <sup>-</sup>
2	1	2-Me	2-Me	88	C <sub>23</sub> H <sub>23</sub> N <sub>3</sub> Cl <sub>3</sub> Cr	55.27	4.64	8.41	54.67	5.13	8.26	2950, 2909, 1577, 1487, 1274, 1229, 1037, 1012, 853, 755	(MALDI): m/z 491 [M - Cl] <sup>+</sup> (ES <sup>+</sup> ): m/z 551 [M - Cl + CH <sub>3</sub> OH] <sup>+</sup> ; (ES <sup>-</sup> ): m/z 553 [M - H] <sup>-</sup>
3	1	2-Et	2-Et	78	C <sub>25</sub> H <sub>27</sub> N <sub>3</sub> Cl <sub>3</sub> Cr	56.88	5.16	7.96	56.67	5.44	7.74	2958, 2925, 2868, 1573, 1483, 1372, 1274, 821, 743	(ES <sup>+</sup> ): m/z 551 [M - Cl + CH <sub>3</sub> OH] <sup>+</sup> ; (ES <sup>-</sup> ): m/z 553 [M - H] <sup>-</sup>
4	1	2-Pr	2-Pr	76	C <sub>27</sub> H <sub>31</sub> N <sub>3</sub> Cl <sub>3</sub> Cr	58.34	5.62	7.56	57.90	5.66	7.37	2962, 2868, 1581, 1487, 1271, 1041, 1009, 858, 755	(ES <sup>+</sup> ): m/z 551 [M - Cl + CH <sub>3</sub> OH] <sup>+</sup> ; (ES <sup>-</sup> ): m/z 553 [M - H] <sup>-</sup>
5	1	2-tBu	2-tBu	72	C <sub>29</sub> H <sub>35</sub> N <sub>3</sub> Cl <sub>3</sub> Cr <sup>d</sup>	59.65	6.04	7.20	59.26	6.13	7.37	2954, 2909, 1699, 1581, 1487, 1368, 1278, 809, 755	(ES <sup>+</sup> ): m/z 551 [M - Cl + CH <sub>3</sub> OH] <sup>+</sup> ; (ES <sup>-</sup> ): m/z 553 [M - H] <sup>-</sup>
6	1	2,6-Me <sub>2</sub>	2,6-Me <sub>2</sub>	69	C <sub>25</sub> H <sub>27</sub> N <sub>3</sub> Cl <sub>3</sub> Cr <sup>d</sup>	56.88	5.16	7.96	56.58	4.83	7.81	2954, 2909, 1585, 1458, 1270, 1217, 1009, 858	(ES <sup>+</sup> ): m/z 380 [M - 3Cl + 2CH <sub>3</sub> OH] <sup>+</sup> ; (ES <sup>-</sup> ): m/z 388 [M - Cl] <sup>-</sup>
7	1	2,5-tBu <sub>2</sub>	2,5-tBu <sub>2</sub>	73	C <sub>37</sub> H <sub>31</sub> N <sub>3</sub> Cl <sub>3</sub> Cr	63.83	7.38	6.04	63.36	7.49	5.83	2958, 2901, 1581, 1495, 1466, 1372, 1274, 927, 825	(ES <sup>+</sup> ): m/z 380 [M - 3Cl + 2CH <sub>3</sub> OH] <sup>+</sup> ; (ES <sup>-</sup> ): m/z 388 [M - Cl] <sup>-</sup>
8	2	2,6-Me <sub>2</sub>	N.A.	70	C <sub>17</sub> H <sub>18</sub> N <sub>2</sub> OCl <sub>3</sub> Cr	48.08	4.27	6.60	47.84	4.67	5.90	2946, 2901, 1622, 1577, 1466, 1360, 1258, 1213, 1099, 821, 772, 629	(ES <sup>+</sup> ): m/z 380 [M - 3Cl + 2CH <sub>3</sub> OH] <sup>+</sup> ; (ES <sup>-</sup> ): m/z 388 [M - Cl] <sup>-</sup>
9	2	2,6-Pr <sub>2</sub>	N.A.	77	C <sub>21</sub> H <sub>26</sub> N <sub>2</sub> OCl <sub>3</sub> Cr	52.46	5.45	5.83	52.58	5.54	5.71	2966, 2925, 2896, 2863, 1630, 1577, 1368, 1262, 1213, 1041, 804, 633	(ES <sup>+</sup> ): m/z 467 [M - Cl + CH <sub>3</sub> OH] <sup>+</sup> ; (ES <sup>-</sup> ): m/z 435 [M - Cl] <sup>-</sup>
10	2	2-tBu	N.A.	67	C <sub>19</sub> H <sub>22</sub> N <sub>2</sub> OCl <sub>3</sub> Cr	50.40	4.90	6.19	50.50	5.40	6.10	2954, 2909, 2868, 1699, 1581, 1483, 1368, 1278, 813, 755	(ES <sup>+</sup> ): m/z 467 [M - Cl + CH <sub>3</sub> OH] <sup>+</sup> ; (ES <sup>-</sup> ): m/z 435 [M - Cl] <sup>-</sup>
11	1	2,4,6-Me <sub>3</sub>	4-tBu	83	C <sub>28</sub> H <sub>33</sub> N <sub>3</sub> Cl <sub>3</sub> Cr	59.01	5.84	7.37	58.93	6.00	6.93	2958, 2921, 2868, 1580, 1503, 1479, 1274, 1037, 858, 821, 567	(ES <sup>+</sup> ): m/z 565 [M - Cl + CH <sub>3</sub> OH] <sup>+</sup> ; (ES <sup>-</sup> ): m/z 567 [M - H] <sup>-</sup>
12	1	2,4,6-Me <sub>3</sub>	2-Me	81	C <sub>25</sub> H <sub>27</sub> N <sub>3</sub> Cl <sub>3</sub> Cr	56.88	5.16	7.96	57.18	5.20	7.44	2945, 2917, 1573, 1483, 1381, 1274, 1229, 1041, 821, 751	(ES <sup>+</sup> ): m/z 497 [M - 3Cl + 2CH <sub>3</sub> OH] <sup>+</sup> ; (ES <sup>-</sup> ): m/z 505 [M - Cl] <sup>-</sup>
13	1	2,4,6-Me <sub>3</sub>	2-Et	94	C <sub>26</sub> H <sub>29</sub> N <sub>3</sub> Cl <sub>3</sub> Cr	57.63	5.39	7.75	57.20	5.37	7.47	2819, 2590, 1593, 1520, 1483, 1446, 858, 760	(ES <sup>+</sup> ): m/z 497 [M - 3Cl + 2CH <sub>3</sub> OH] <sup>+</sup> ; (ES <sup>-</sup> ): m/z 505 [M - Cl] <sup>-</sup>
14	1	2,6-Pr <sub>2</sub>	2,6-Pr <sub>2</sub>	56	C <sub>33</sub> H <sub>43</sub> N <sub>3</sub> Cl <sub>3</sub> Cr <sup>d</sup>	61.92	6.77	6.56	61.64	6.87	6.44		(ES <sup>+</sup> ): m/z 497 [M - 3Cl + 2CH <sub>3</sub> OH] <sup>+</sup> ; (ES <sup>-</sup> ): m/z 505 [M - Cl] <sup>-</sup>

<sup>a</sup> Catalyst type, as shown by the general structures in Scheme 1. <sup>b</sup> Substitution pattern of imino aryl rings according to Scheme 1; for example, 2-H represents unsubstituted aryl rings for a Type 1 complex. <sup>c</sup> The precatalyst complexes were prepared on a 300 mg scale, using 1.1 equiv of the ligand. <sup>d</sup> This complex was previously reported in ref 11. <sup>e</sup> Electrospray spectrometry is performed using a methanol solution of the complex, which causes coordination of methanol to chromium with concomitant chlorine loss in some instances. Representative samples of each catalyst type were analyzed by the techniques indicated.

run at least twice or until comparable results could be obtained.

The studies examining the impact of Al:Cr ratio on product properties (Table 2 and Figure 4) and the comparative reactivity between chromium(II) and chromium(III) complexes (Table 5 and Figure 7) were carried out in toluene and used commercial MAO (10% in toluene) provided by Albemarle.

**Product Analysis.** The aluminum cocatalysts were removed by the addition of acidified methanol and subsequent decantation and/or filtration of the products. After removal of the cocatalysts, the products were analyzed by gas chromatography (GC) using tridecane as internal standard.

**X-ray Crystallography.** Single-crystal specimens selected for crystallographic characterization were mounted on thin glass fibers and transferred to an Enraf-Nonius CAD4 (6', 6) or a Bruker-Nonius MACH3S (5') diffractometer equipped with graphite-monochromated Mo K $\alpha$  radiation ( $\lambda = 0.71073 \text{ \AA}$ ) for data collections at ambient temperature. Unit cell constants were determined from a least-squares refinement of the setting angles of 25 machine-centered reflections located using an automated search routine. Intensity data were collected using the  $\omega/2\theta$  scan technique to a maximum  $2\theta$  value of  $50^\circ$ . When necessary, absorption corrections were applied using azimuthal scans of several intense reflections. The data were corrected for Lorentz and polarization effects and converted to structure factors using the teXsan for Windows crystallographic software package.<sup>27</sup> Space groups were determined based on systematic absences and intensity statistics. Structures were solved by direct methods or by the Patterson method, which provided the positions of most of the non-hydrogen atoms. The remaining non-hydrogen atoms were located after several cycles of structure expansion and full-matrix least-squares refinement (on  $F^2$ ). In addition to the chromium complex, two CH<sub>3</sub>CN solvates were identified in the lattice of 5'. Hydrogen atoms were added geometrically. All non-hydrogen atoms were refined using anisotropic displacement parameters, while hydrogen atoms were refined as riding atoms with group isotropic displacement parameters. Structure solution and refinement was performed using the SHELXTL suite of programs running on a Pentium PC.<sup>28</sup>

**Acknowledgment.** B.L.S. acknowledges Ray Rios, Eric Fernandez, and A. J. Marcucci for performing many of the batch reactor studies. M.J.C. acknowledges the donors of the Petroleum Research Fund, administered by the American Chemical Society (Grant 37885-GB3), Research Corporation (Cottrell College Science Award), and the University of Wisconsin—Eau Claire for financial support of this research. J.A.H. acknowledges the support of the National Science Foundation (CHE-0078746) and the University of Wisconsin—Eau Claire. Instrumentation for infrared analyses was obtained with the support of the National Science Foundation MRI (CHE-0216058). We also thank Nick Robertson for experimental assistance, Albemarle for kindly providing MAO, W. R. Grace (Davison Catalyst Division) for polymer GPC and <sup>13</sup>C NMR analyses, and Paul DeLauriers (CPChem) for GPC analyses.

**Supporting Information Available:** Complete X-ray crystallographic information in CIF format; GPC traces for the polymers reported in Table 1. This material is available free of charge via the Internet at <http://pubs.acs.org>.

## References and Notes

- (1) (a) Britovsek, G. J. P.; Gibson, V. C.; Wass, D. F. *Angew. Chem., Int. Ed. Engl.* **1999**, *38*, 428 and references therein. (b) Gibson, V. C.; Spitzmesser, S. K. *Chem. Rev.* **2003**, *103*, 283–316.
- (2) Supported chromium oxide catalysts: (a) Hogan, J. P. *J. Polym. Sci., Polym. Chem. Ed.* **1970**, *8*, 2637–2652. (b) McDaniel, M. P. *Adv. Catal.* **1985**, *33*, 47–96. Supported chromocene catalysts: (c) Karol, F. J.; Karapinka, G. L.; Wu, C.; Dow, A. W.; Johnson, R. N.; Carrick, W. L. *J. Polym. Sci., Polym. Chem. Ed.* **1972**, *10*, 2621–2637. (d) Karol, F. J.; Brown, G. L.; Davison, J. M. *J. Polym. Sci., Polym. Chem. Ed.* **1973**, *11*, 413–424.
- (3) In addition to the examples of chromium polymerization catalysts shown in Figure 1 in this report, the growing number of chromium systems that are selective for producing 1-hexene must also be noted. Although such a discussion is beyond the scope of this work, a few noteworthy references are hereby included: (a) McGuinness, D. S.; Wasserscheid, P.; Keim, W.; Morgan, D.; Dixon, J. T.; Bollmann, A.; Maumela, H.; Hess, F.; Englert, U. *J. Am. Chem. Soc.* **2003**, *125*, 5272. (b) McGuinness, D. S.; Wasserscheid, P.; Keim, W.; Hu, C.; Englert, U.; Dixon, J. T.; Grove, C. *Chem. Commun.* **2003**, 334. (c) Carter, A.; Cohen, S. A.; Cooley, N. A.; Murphy, A.; Scutt, J.; Wass, D. F. *Chem. Commun.* **2002**, 858. (d) Reagan, W. K.; Pettijohn, T. M.; Freeman, J. W. (Phillips Petroleum) U.S. Patent 5523507, 1996. (e) Wu, F.-J. (Amoco) U.S. Patent 5811618, 1998. (f) Briggs, J. R. (Union Carbide) U.S. Patent 4668838, 1987.
- (4) (a) Leesubcharoen, S.; Lam, K.-C.; Concolino, T. E.; Rheingold, A. L.; Theopold, K. H. *Organometallics* **2001**, *20*, 182. (b) Heintz, R. A.; Leesubcharoen, S.; Liable-Sands, L. M.; Rheingold, A. L.; Theopold, K. H. *Organometallics* **1998**, *17*, 5477. (c) Theopold, K. H. *Eur. J. Inorg. Chem.* **1998**, 15. (d) Theopold, K. H. *Chemtech* **1997**, October, 26. (e) White, P. A.; Calabrese, J.; Theopold, K. H. *Organometallics* **1996**, *15*, 5473. (f) Liang, Y.; Yap, G. P. A.; Rheingold, A. L.; Theopold, K. H. *Organometallics* **1996**, *15*, 5284.
- (5) Baralt, E. J.; Carney, M. J.; Cole, J. B. (Chevron Chemical) U.S. Patent 5780698, 1998.
- (6) (a) Kim, W.-K.; Fevola, M. J.; Liable-Sands, L. M.; Rheingold, A. L.; Theopold, K. H. *Organometallics* **1998**, *17*, 4541. (b) Gibson, V. C.; Maddox, P. J.; Newton, C.; Redshaw, C.; Solan, G. A.; White, A. J. P.; Williams, D. J. *Chem. Commun.* **1998**, 1651. (c) Gibson, V. C.; Newton, C.; Redshaw, C.; Solan, G. A.; White, A. J. P.; Williams, D. J. *J. Chem. Soc., Dalton Trans.* **1999**, 827. (d) Coles, M. P.; Dalby, C. I.; Gibson, V. C.; Little, I. R.; Marshall, E. L.; Ribeiro da Costa, M. H.; Mastroianni, S. *J. Organomet. Chem.* **1999**, *591*, 78. (e) Jensen, V. R.; Børve, K. J. *Organometallics* **2001**, *20*, 616.
- (7) Matsunaga, P. T. (Exxon Chemical) WO9957159, 1999.
- (8) (a) Jensen, V. R.; Angermund, K.; Jolly, P. W. *Organometallics* **2000**, *19*, 403. (b) Döhring, A.; Göhre, J.; Jolly, P. W.; Kryger, B.; Rust, J.; Verhovnik, G. P. *J. Organometallics* **2000**, *19*, 388. (c) Emrich, R.; Heinemann, O.; Jolly, P. W.; Krüger, C.; Verhovnik, G. P. *J. Organometallics* **1997**, *16*, 1511.
- (9) Devore, D.; Feng, S. S.; Frazier, K. A.; Patton, J. T. (Dow Chemical) WO0069923, 2000.
- (10) Köhn, R. D.; Haufe, M.; Mihan, S.; Lilje, D. *Chem. Commun.* **2000**, 1927.
- (11) (a) Esteruelas, M. A.; López, A. M.; Méndez, L.; Oliván, M.; Oñate, E. *Organometallics* **2003**, *22*, 395. (b) Small, B. L.; Marcucci, A. J. (Chevron Phillips Chemical) WO03054038, 2003.
- (12) Aleya, E. C.; Merrell, P. H. *Synth. React. Inorg. Metal-Org. Chem.* **1974**, *4*(6), 535.
- (13) (a) Ittel, S. D.; Johnson, L. K.; Brookhart, M. *Organometallics* **2000**, *19*, 1169. (b) Small, B. L.; Brookhart, M. *Polym. Prepr., Am. Chem. Soc. Div. Polym. Chem.* **1998**, *39*, 213. (c) Britovsek, G. J. P.; Gibson, V. C.; Kimberley, B. S.; Maddox, P. J.; McTavish, S. J.; Solan, G. A.; White, A. J. P.; Williams, D. J. *Chem. Commun.* **1998**, 849. (d) Small, B. L.; Brookhart, M.; Bennett, A. M. A. *J. Am. Chem. Soc.* **1998**, *120*, 4049. (e) Small, B. L.; Brookhart, M. *J. Am. Chem. Soc.* **1998**, *120*, 7143. (f) Britovsek, G. J. P.; Bruce, M.; Gibson, V. C.; Kimberley, B. S.; Maddox, P. J.; Mastroianni, S.; McTavish, S. J.; Redshaw, C.; Solan, G. A.; Strömberg, S.; White, A. J. P.; Williams, D. J. *J. Am. Chem. Soc.* **1999**, *121*, 8728. (g) Bennett, A. M. A. *Chemtech* **1999**, *29*(7), 24. (h) Britovsek, G. J. P.; Mastroianni, S.; Solan, G. A.; Baugh, S. P. D.; Redshaw, C.; Gibson, V. C.; White, A. J. P.; Williams, D. J.; Elsegood, M. R. *J. Chem. Eur. J.* **2000**, *6*, No. 12, 2221.
- (14) Syntheses for the Type 2 unsymmetrical ligands, as well as their iron and cobalt transition-metal complexes, can be found in the following references: (a) Bennett, A. M. A. (DuPont) U.S. Patent 5955555, 1999. (b) Small, B. L.; Brookhart, M. *Macromolecules* **1999**, *32*, 2120. (c) Gibson, V. C.; Kimberley, B. S.; Solan, G. A. (BP) WO0020427, 2000. (d) Sommazzi, A.; Milani, B.; Proto, A.; Corso, G.; Mestroni, G.; Masi, F. (Enichem) WO0110875, 2001. (e) de Boer, E. J. M.; Deuling,

- H. H.; van der Heijden, H.; Meijboom, N.; van Oort, A. B. (Shell) W00158874, 2001.
- (15) Modified methylalumoxane refers to MMAO-3A (Al 7% by wt), an isobutyl-modified MAO supplied by Akzo Nobel.
- (16) The activity of the 2-*tert*-butyl complex **5** in entry 5 of Table 3 agrees reasonably well with the activity reported in ref 11a.
- (17) To determine whether the 2-butene was being generated directly by the dimerization reaction or in a separate isomerization step, MMAO-activated **1** was tested for the isomerization of 1-hexene and found to be a potent selective isomerization catalyst for converting the 1-olefin to the 2-olefin.
- (18) (a) Johnson, L. K.; Killian, C. M.; Brookhart, M. *J. Am. Chem. Soc.* **1995**, *117*, 6414. (b) Killian, C. M.; Johnson, L. K.; Tempel, D. J.; Brookhart, M. *J. Am. Chem. Soc.* **1996**, *118*, 11664.
- (19) (a) Sugiyama, H.; Aharonian, G.; Gambarotta, S.; Yap, G. P. A.; Budzelaar, P. H. M. *J. Am. Chem. Soc.* **2002**, *124*, 12268. (b) Reardon, D.; Aharonian, G.; Gambarotta, S.; Yap, G. P. A. *Organometallics* **2002**, *21*, 786.
- (20) Reardon, D.; Conan, F.; Gambarotta, S.; Yap, G.; Wang, Q. *J. Am. Chem. Soc.* **1999**, 9318.
- (21) Talzi, E. P.; Babushkin, D. E.; Semikolenova, N. V.; Zudin, V. N.; Zakharov, V. A. *Kinet. Catal.* **2001**, *42* (2), 147.
- (22) (a) Gibson, V. C.; Humphries, M. J.; Tellman, K. P.; Wass, D. F.; White, A. J. P.; Williams, D. J. *Chem. Commun.* **2001**, 2252. (b) Kooistra, T. M.; Knijnenburg, Q.; Smits, J. M. M.; Horton, A. D.; Budzelaar, P. H. M.; Gal, A. W. *Angew. Chem., Int. Ed.* **2001**, *40* (24), 4719.
- (23) (a) Dias, E. L.; Brookhart, M.; White, P. S. *Organometallics* **2000**, *19*, 4995. (b) Dias, E. L.; Brookhart, M.; White, P. S. *Chem. Commun.* **2001**, 423.
- (24) Batch studies of the Cr(II) and Cr(III) systems showed similar activities, product distributions, and product compositions when the same ligand was used with either metal source. To further evaluate the similarity of the Cr(II) and Cr(III) systems, a side-by-side comparison was performed using a Multiclave 10× reactor from Autoclave Engineers. This reactor possesses 10 individual 30 mL cells, with each cell having stirring and temperature control capabilities. A 2.0 mg amount of five different Cr(II) and Cr(III) complexes was activated with MMAO (1000:1 Al:Cr) in heptane (15 mL) and exposed to 13.6 bar of ethylene, fed "on demand" for 30 min. In each case, as in the larger batch studies, the products were the same, depending entirely on the ligand rather than the oxidation state of the precatalyst. The only difference observed was that the Cr(III) complexes appeared to activate slightly faster, which was noted by watching the comparative temperature profiles for the Cr(II) and Cr(III) catalysts, respectively.
- (25) UV-vis studies have been used to study the reaction between alumoxanes and transition-metal complexes in related Fe systems: (a) Luo, H.-K.; Yang, Z.-H.; Mao, B.-Q.; Yu, D.-S.; Tang, R.-G. *J. Mol. Catal. A: Chem.* **2002**, *177*, 195. (b) Britovsek, G. J. P.; Gibson, V. C.; Spitzmesser, S. K.; Tellmann, K. P.; White, A. J. P.; Williams, D. J. *J. Chem. Soc., Dalton Trans.* **2002**, 1159.
- (26) Zuech, E. A. (Phillips Petroleum) U.S. Patent 3726939, 1973.
- (27) *TeXsan for Windows, V 1.02*; Molecular Structure Corp., Inc.: The Woodlands, TX.
- (28) *SHELXTL V. 5.1*; Bruker AXS: Madison, WI.

MA035554B